

# Photoluminescence band of Hf origin in hafnium-implanted silicon in the energy range 700 meV to 950 meV

R. Sachdeva\* and A. A. Istratov

*Department of Materials Science and Engineering, University of California, Berkeley, and Materials Science Division, Lawrence Berkeley National Laboratory, Berkeley, California 94720, USA*

P. N. K. Deenapanray

*Center for Sustainable Energy Systems, The Australian National University, Canberra, Australia 0200*

E. R. Weber

*Department of Materials Science and Engineering, University of California, Berkeley, and Materials Science Division, Lawrence Berkeley National Laboratory, Berkeley, California 94720, USA*

(Received 5 October 2004; revised manuscript received 13 January 2005; published 31 May 2005)

A new photoluminescence (PL) band in the energy range of 700 to 950 meV associated with hafnium implanted in silicon is reported. A shift in the position of photoluminescence peaks observed on the samples implanted with two different isotopes of Hf confirms the Hf-related origin of the observed photoluminescence band. Activation of the Hf-optical centers requires a 1000 °C anneal step. The intensity of the PL lines depends on the cooling conditions. The spectrum consists of 5 peaks in the rapidly quenched sample as opposed to 21 in the slowly cooled sample. Temperature- and excitation power-dependent PL measurements were performed to identify their nature. The 943.8 meV line was associated with an exciton complex, while the 896.6 meV line originates from impurity bound exciton. The 896.6 meV emission line appears to be related to a Hf-related deep level defect at  $E_C-0.22$  eV, the 845 meV line to a deep level defect at  $E_C-0.27$  eV. The pressure measurements indicate that the 845 meV peak could be an internal transition. It is also found that oxygen coimplantation enhances the PL intensity in rapidly quenched samples.

DOI: 10.1103/PhysRevB.71.195208

PACS number(s): 71.20.Be, 71.20.Mq, 71.55.-i

## I. INTRODUCTION

There has been much interest in replacing silicon dioxide in CMOS transistors and using gate dielectric films with high dielectric constants. The area of advanced gate dielectrics has gained considerable attention recently. Among the high- $k$  dielectrics  $ZrO_2$ ,  $HfO_2$ ,  $Ta_2O_5$ , and  $Al_2O_3$ , etc., have high dielectric constants, but the most promising in terms of meeting the requirements and improving the performance of Si devices appears to be  $HfO_2$ .<sup>1,2</sup> The activation of implanted dopants such as phosphorus or boron in silicon require high-temperature anneals. A high-temperature anneal could lead to metal (Hf) associated with the dielectric film ( $HfO_2$ ) to diffuse into the near-surface device layer of the sample. Therefore, it becomes important to understand the electrical and optical properties of Hf in Si. Electrical levels of Hf in Si observed in samples doped with Hf during crystal growth were reported by Lemke.<sup>3</sup> However, there are hardly any data on optical properties of Hf in Si. In our investigation, we report observation of a PL signal of Hf in Si in the energy range of 700 to 950 meV and describe the general features of the emission spectra, its dependence on the quenching process, and the influence of oxygen concentration on luminescence.

## II. EXPERIMENTAL PROCEDURES

$N$ -type Czochralski (CZ) silicon wafers with a resistivity of 5–10  $\Omega$  cm were implanted with hafnium at an energy of

50 keV and dose of  $10^{13}$   $cm^{-2}$ . Some  $p$ -type CZ samples were also implanted and showed similar results as  $n$ -type silicon. The implantation profile showed a hafnium peak concentration of  $10^{18}$   $cm^{-3}$  as measured by secondary ion mass spectrometry (SIMS). In the as-implanted samples, the crystalline quality was good as confirmed by Rutherford back scattering (RBS) which could be expected because the implant was a nonamorphizing low-dose implant ( $10^{13}$   $cm^{-2}$ ).<sup>4</sup> Unfortunately, the Hf concentration in these samples was below the detection limit of RBS. Additionally, samples contaminated during growth from the silicon melt (courtesy of H. Lemke) were also measured, but no PL signal was observed.

The source of the ion implanter used in this study produces negative ions by cesium sputtering. Since the yield of  $Hf^-$  is poor, Hf has been implanted in the  $HfO^-$  molecular form, where it is expected to break up into Hf and O.<sup>5-8</sup> The isotope  $^{180}Hf$  has been implanted in the silicon samples, with the exception of the experiments described in Sec. III B, where samples implanted with  $^{178}Hf$  and  $^{180}Hf$  were compared. To study the effect of oxygen concentration, several samples were additionally implanted with oxygen.

Samples were annealed in a horizontal furnace in Ar ambient in three steps: 650 °C for 30 min, then 1000 °C for 3 h, and then cooled to room temperature. The first step is often used to anneal out implantation-induced damage and restore crystallinity.<sup>9</sup> The second step (1000 °C) is needed to activate Hf. Two different cooling rates were used to cool the sample from the annealing temperature of 1000 °C to room

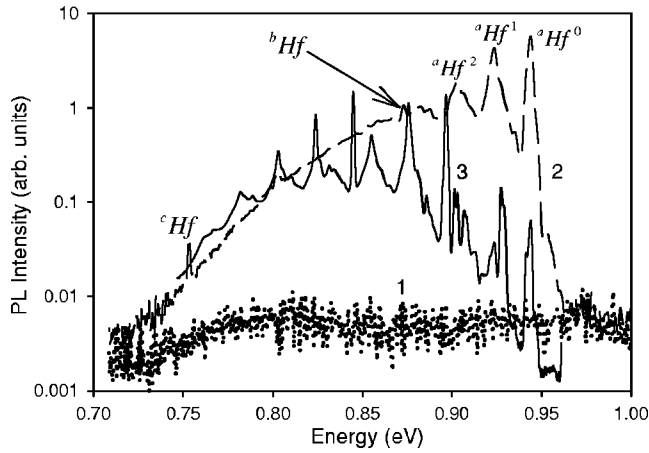


FIG. 1. The PL spectra of Hf in Si. The dotted line (curve 1) represents the sample which was annealed at 650 °C for 30 min. The dashed line (curve 2) is the sample which was annealed at 650 °C for 30 min, 1000 °C for 3 h, and rapidly quenched. The solid line (curve 3) indicates the sample that was annealed at 650 °C for 30 min, 1000 °C for 3 h, and slowly cooled.

temperature. The first one, slow furnace cool, was implemented by shutting down the furnace and allowing sample to cool to room temperature, which took about 30 min. The second technique, rapid quench, involves removing the sample at 1000 °C and dropping it on an Al plate heat sink.

Photoluminescence (PL) measurements were performed in a closed-cycle helium cryostat at 12 K unless noted otherwise. The PL was excited by a cw argon-ion laser (20 mW at the sample surface unless noted otherwise) with a wavelength of 514.5 nm and detected with a Ge detector cooled by liquid nitrogen.

### III. RESULTS AND DISCUSSION

#### A. Dependence of PL spectra on cooling conditions

Figure 1 shows PL spectra for three samples. Curve 1 (dotted line) represents PL spectrum for a Hf-implanted sample annealed at 650 °C for 30 min. Curve 2 (dashed line) is PL signal for a sample that was annealed at 650 °C for 30 min, 1000 °C for 3 h, and rapidly quenched. Curve 3 (solid line) shows a sample which was annealed at 650 °C for 30 min, 1000 °C for 3 h, and cooled slowly to room temperature. It is clear that the 1000 °C annealing step is critical to the activation of the optical centers, and that the quenching process plays a significant role in determining the PL spectrum. The quenching process has also been reported<sup>10</sup> to be a dominant factor in determining the PL spectrum of silicon lightly doped with copper. For curve 2, five distinct peaks are observed on top of the broad band centered at 0.85 eV. From high to low energy, these peaks are labeled as  $^a\text{Hf}^0$ ,  $^a\text{Hf}^1$ ,  $^a\text{Hf}^2$ ,  $^b\text{Hf}$ , and  $^c\text{Hf}$ . In this notation, the left superscript indicates the line system and the right superscript denotes the number of phonons involved. The distances between  $^a\text{Hf}^0$ ,  $^a\text{Hf}^1$ , and  $^a\text{Hf}^2$  are similar, indicating that  $^a\text{Hf}^1$  and  $^a\text{Hf}^2$  are likely to be phonon replicas of  $^a\text{Hf}^0$ . The lines, their energies, their tentative system groupings,

TABLE I. A compilation of all sharp lines observed in the Hf spectrum for the rapidly quenched and the slowly cooled samples. The labeling is explained in the text. The implanted species was  $^{180}\text{Hf}$ .

Line	Energy (meV)	Description	$\Delta E(\text{meV})$	
			spectral	Phonon (meV)
$^a\text{Hf}^0$	943.8	Zero-phonon line	...	
$^a\text{Hf}^1$	923.6	Phonon replica	20.2	20.2
$^a\text{Hf}^2$	902.6	Phonon replica	41.2	21.0
$^b\text{Hf}$	873	Peak		
$^c\text{Hf}$	753.2	Peak		
$^d\text{Hf}^0$	896.6	Zero-phonon line		
$^d\text{Hf}^1$	875.8	Phonon replica	20.8	20.8
$^d\text{Hf}^2$	855	Phonon replica	41.6	20.8
$^d\text{Hf}^3$	834.1	Phonon replica	62.5	20.9
$^e\text{Hf}^0$	845	Zero phonon line		
$^e\text{Hf}^1$	823.9	Phonon replica	21.1	21.1
$^e\text{Hf}^2$	803	Phonon replica	42.0	20.9
$^e\text{Hf}^3$	782.1	Phonon replica	62.9	20.9
$^f\text{Hf}^0$	831.4	Zero phonon line		
$^f\text{Hf}^1$	810.1	Phonon replica	21.3	21.3
$^f\text{Hf}^2$	788.9	Phonon replica	42.5	21.2
$^g\text{Hf}^0$	927.4	Zero phonon line		
$^g\text{Hf}^1$	906.8	Phonon replica	20.6	20.6
$^h\text{Hf}$	941.5	Peak		
$^i\text{Hf}$	935	Peak		
$^j\text{Hf}$	912.4	Peak		
$^k\text{Hf}$	903.1	Peak		
$^l\text{Hf}$	901.3	Peak		
$^m\text{Hf}$	885.8	Peak		

and the energy difference between the phonon replica and its zero phonon line of a particular line system ( $\Delta E$ ) are tabulated in Table I.

Evidently, the broad band in the upper half of the spectra drops in magnitude for slowly cooled sample 3 in Fig. 1. The PL spectrum of curve 3 displays 21 lines compared to 5 for curve 2. Since the lines are so numerous, they have not been labeled in Fig. 1, and are shown on a more detailed scale in Fig. 2. Two lines ( $^a\text{Hf}^0$  and  $^a\text{Hf}^1$ ) are common to both the PL spectra of curves 2 and 3. Two new systems with three phonon replicas are observed after slow cool,  $^d\text{Hf}$  (zero-phonon line at 896.6 meV) and  $^e\text{Hf}$  (zero-phonon line at 845 meV). Another PL peak found at 831.4 meV ( $^f\text{Hf}^0$ ) has two phonon replicas. Since the values of  $\Delta E$  for phonon replicas of  $^a\text{Hf}$ ,  $^d\text{Hf}$ ,  $^e\text{Hf}$ ,  $^f\text{Hf}$ , and  $^g\text{Hf}$  listed in Table I are very similar, it appears that they are due to the same phonon with  $20.9 \pm 0.6$  meV, which matches within the error margins the  $21.3 \pm 0.5$  meV transverse acoustic (TA) phonon.<sup>11,12</sup> Additionally, there are six peaks in the PL spectrum of the slowly cooled sample labeled as  $^h\text{Hf}$ ,  $^i\text{Hf}$ ,  $^j\text{Hf}$ ,  $^k\text{Hf}$ ,  $^l\text{Hf}$ , and  $^m\text{Hf}$

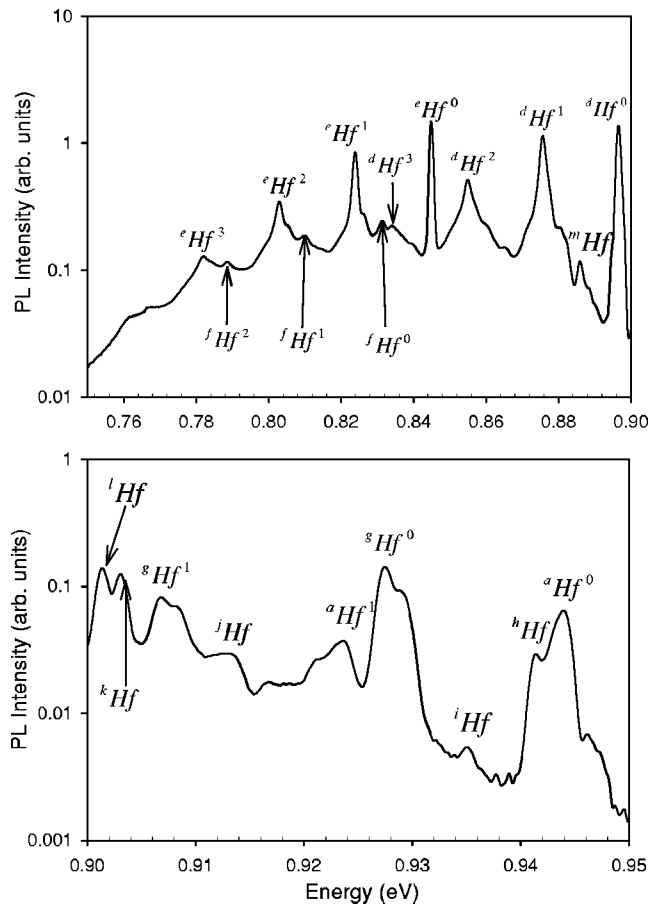


FIG. 2. Detailed PL spectrum [(a) lower half, and (b) upper half] of sample annealed at 650 °C for 30 min, then 1000 °C for 3 h, and then slowly cooled.

with relatively low PL signal. They are given no right-sided superscripts because they do not appear to have any phonon replicas (or the intensities of these replicas are too low to be detected).

Since there are two PL spectra obtained depending on the quenching process, it was interesting to see whether the PL spectrum of a rapidly quenched sample can be converted to the spectrum of a slowly cooled sample by a short reanneal. The rapidly quenched sample (curve 2 in Fig. 1) was further annealed in the horizontal furnace at 1000 °C for 30 min and allowed to cool slowly to room temperature. PL was measured again and a curve similar to spectrum 3 was obtained. Likewise, it was found that if a slowly cooled sample showing spectrum 3 was reannealed at 1000 °C for 30 min and then rapidly quenched, a PL spectrum very similar to spectrum 2 was observed. Therefore, the PL spectrum of a slowly cooled sample can be changed into the PL spectrum of a rapidly quenched sample simply by a reanneal, and vice versa.

In Fig. 1, the  $^a\text{Hf}^0$  peak is about two orders of magnitude weaker in slowly cooled sample than the rapidly quenched sample. Crystalline quality of the silicon has been observed<sup>13–15</sup> to adversely affect the luminescence of Er. However, RBS measurements revealed no difference in the crystalline quality of the rapidly quenched and the slowly

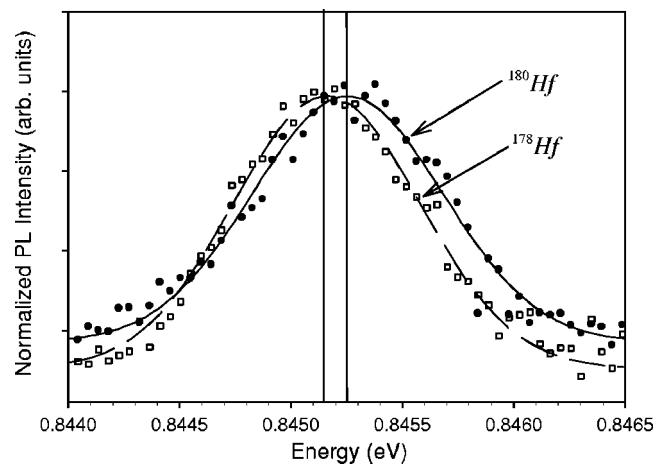


FIG. 3. High-resolution PL spectra of the  $^e\text{Hf}^0$  line for samples implanted with  $^{178}\text{Hf}$  and  $^{180}\text{Hf}$ , respectively. The solid and dashed line are Gaussian fits to the experimental points. The vertical lines indicate positions of the peaks estimated from the fit.

cooled samples. Therefore, it is likely that the microscopic structure of the Hf-implanted samples changes depending on the cooling rate of the samples. One can speculate that in the case of a rapid cooling, higher Hf concentration gets quenched in the dissolved state (which could be interstitial or substitutional), and it is possible that the dominant peak in the PL spectrum,  $^a\text{Hf}^0$ , is due to these isolated Hf species. Since dissolved hafnium can travel longer distances in the slowly cooled samples, it is likely that these samples have a higher fraction of complexes and thus more small lines appear (see Fig. 1), while the density of dissolved species which give rise to the  $^a\text{Hf}^0$  emission decreases.

### B. Isotope substitution

To unambiguously identify hafnium as the source of the PL signal obtained in our experiments, we compared PL spectra of two samples implanted with  $^{178}\text{Hf}$  and  $^{180}\text{Hf}$ , respectively. The implanted samples were annealed at 650 °C for 30 min, 1000 °C for 3 h, and then slowly cooled. The  $^e\text{Hf}^0$  line [the strongest line in the spectra of these samples; see Fig. 2(a)] was measured with a small step size and highest resolution possible for our experimental setup. Figure 3 shows the experimental points for both spectra, their Gaussian fits, and the center point for each of the fitted curves. The center points of spectrum peaks for  $^{178}\text{Hf}$  and  $^{180}\text{Hf}$  are 845.15 and 845.25 meV, respectively. An isotope shift of  $0.1 \pm 0.02$  meV is clearly visible. The lighter isotope has a lower transition energy as expected for an oscillator model. This isotope shift is consistent with shifts observed in the literature for other metals in Si, such as for copper and zinc. For copper, the shift between  $^{63}\text{Cu}$  and  $^{65}\text{Cu}$  is 0.08 meV,<sup>16</sup> and for zinc, the shift between  $^{64}\text{Zn}$  and  $^{68}\text{Zn}$  is 0.1 meV.<sup>17</sup> These measurements provide direct evidence that the observed luminescence is indeed hafnium related.

### C. Temperature-dependent PL

The variation of the emission intensity with temperature under continuous excitation is a measure of luminescent ef-

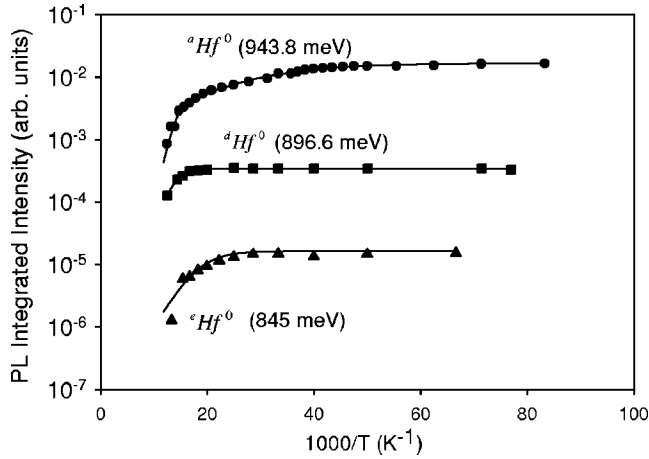


FIG. 4. Temperature dependence of the  ${}^a\text{Hf}^0$ ,  ${}^d\text{Hf}^0$ , and  ${}^e\text{Hf}^0$  line intensities. The symbols are the experimental points. The solid lines represent the fit.

efficiency and provides a key to understanding the mechanism of luminescence. Three peaks with the strongest PL signal at 12 K,  ${}^a\text{Hf}^0$  (see Fig. 1),  ${}^d\text{Hf}^0$ , and  ${}^e\text{Hf}^0$  [see Fig. 2(a)], were chosen for analysis of temperature dependence of PL intensity. Figure 4 shows the integrated intensity against reciprocal temperature for  ${}^a\text{Hf}^0$ . If we assume that an exciton complex is involved in the luminescence process, the intensity can be described with the following formula:<sup>18</sup>

$$I(T) = \frac{I(0)}{\left[ 1 + \sum_{i=1}^N C_i \exp\left(-\frac{E_i}{k_B T}\right) \right]}, \quad (1)$$

where  $I(T)$  is the luminescence intensity at temperature  $T$ ,  $I(0)$  is the intensity at 0 K, and  $k_B$  is the Boltzmann constant.

This formula is based on a model that photoluminescence stems from an exciton complex having  $N$  excited states at energies  $E_i$  higher than the ground state  $E_0$ . These energies are associated with the dissociation of the impurity-exciton complex. There are various channels of dissociation.<sup>18</sup> One is simply for the bound exciton to become a free exciton. A second way is for the complex to dissociate, resulting in one free electron and one free hole. Another mechanism results in one free hole, and the fourth process involves emitting two free holes and one free electron.  $C_i$  is the degeneracy ratio of level  $i$  to the ground state ( $C_i = g_i/g_0$ , where  $g_i$  and  $g_0$  are degeneracies of levels  $E_i$  and  $E_0$ ) and is also called coupling coefficient. There are two important assumptions under which this formula was derived. The first assumption is that the total number of excitons in the system is temperature independent and hence remains constant. The second assumption is that the occupation of the different exciton levels is temperature dependent.

In 1947, Williams and Eyring<sup>19</sup> suggested the simplest form of Eq. (1) with  $N=1$ , i.e., with a one-step activation process with exciton at ground level. In 1971, Bimberg *et al.*<sup>18</sup> showed that the formula with  $N=1$  could not explain the behavior of excitons bound to donors in GaAs and GaP, and expanded the model to an impurity exciton complex as-

sociated with three energy levels: a ground-state energy  $E_0$  and excited states with excess energies  $E_1$  and  $E_2$ . In 1982, Eq. (1) was extended to a system with four levels,  $E_0$ ,  $E_1$ ,  $E_2$ ,  $E_3$  to explain temperature-dependent luminescence intensity decay of copper pairs in silicon.<sup>16</sup>

With our experimental results in Fig. 4, we tried fitting our data with  $N=1, 2, 3$ , and 4, but only the double exponential gave a good fit. A fit of the data (for the 943.8 meV emission line,  ${}^a\text{Hf}^0$ ) yields  $E_1=8.95$  meV and  $E_2=85.4$  meV, and  $C_1=15.8$  and  $C_2=3.86 \times 10^6$ , respectively. The physical meaning behind the energies is that, if we assume the mechanism for the luminescence decay for center  ${}^a\text{Hf}^0$  constitutes an impurity exciton complex, then that complex has three energy levels: a ground state of energy  $E_0$ , where it is bound, and two higher states of energies 8.95 and 85.4 meV above ground state where it is dissociated. Since the degeneracy ratio  $C_2$  is so high, this is the band into which the ionization will likely occur. Thus, the relevant ionization energy from the exciton ground state is  $E_A=E_2=85.4$  meV. Weber *et al.*<sup>16</sup> found a good correlation between the residual one-particle energy, calculated as  $E_t=E_g-h\nu-E_A$  (where  $h\nu$  is the energy of zero-phonon line,  $E_g$  is the band gap, and  $E_t$  is the electron binding energy), and corresponding energy levels determined from deep-level transient spectroscopy (DLTS) for Cu pairs and CrB pairs. We performed the same calculation with thermal ionization energy of 85.4 meV, from which a residual one-particle binding energy of  $E_t=140$  meV (for the  ${}^a\text{Hf}^0$  PL line) results. Lemke,<sup>3</sup> using DLTS, determined two Hf-related energy levels close to this value at  $E_C-0.10$  eV and  $E_C-0.17$  eV in the upper half of the silicon band gap. Both of these energies are close (within 0.03 to 0.04 eV) to  $E_t$  obtained from our optical measurement, but neither of the two levels matches our calculated  $E_t$  exactly; therefore, it is not possible to identify this optical transition with a particular deep level. We made an attempt to measure DLTS on the rapidly quenched sample but, due to carrier freezeout in Hf-contaminated samples, the capacitance became negligible below 200 K; consequently, the measurements could not be performed at temperatures sufficiently low to detect energy levels around  $E_C-0.14$  eV.

The slowly cooled sample has two other zero phonon peaks with sufficiently high intensity to study them in detail,  ${}^d\text{Hf}^0$  and  ${}^e\text{Hf}^0$  at 896.6 and 845 meV, respectively.

Temperature dependence of PL intensity performed on  ${}^d\text{Hf}^0$  (896.6 meV) is presented in Fig. 4. In this case, only a single exponential [Eq. (1)] was necessary to fit the experimental points, and the relevant ionization energy of  $E_A=51.5$  meV was obtained. From this, a residual one-particle binding energy of  $E_t=0.222$  eV can be calculated. This value is in excellent agreement with  $E_C-0.22$  eV, which is one of the defect levels we found in the slow cool sample using DLTS; furthermore, Lemke *et al.*<sup>3</sup> detected a deep level defect with a similar energy, reported at  $E_C-0.24$  eV.

Figure 4 illustrates the PL integrated intensity for  ${}^e\text{Hf}^0$  (845 meV emission line) and the single exponential fit which yields an activation energy of 28.8 meV. The residual one-particle binding energy of  $E_t=0.296$  eV is close to our value of  $E_C-0.27$  eV obtained from DLTS measurements in the temperature range from 130 to 180 K. The position of data points for the  $E_C-0.27$  eV on the Arrhenius plot correlates

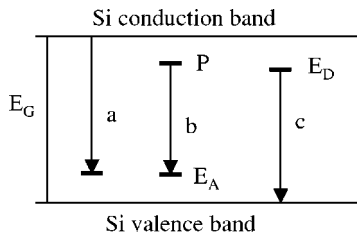


FIG. 5. Illustration of three possible radiative mechanisms: (a) conduction band to deep level; (b) donor-acceptor pair transition; (c) deep level to valence band.

with Lemke's<sup>3</sup> data, which reported, for apparently the same peak, a slightly higher activation energy of  $E_C-0.33$  eV.

As discussed earlier, temperature-dependent PL data for  ${}^a\text{Hf}^0$  yield two activation energies which seem to point to the center being an impurity exciton complex, whereas one-step ionization energy for  ${}^a\text{Hf}^0$  indicates that this emission line may have its origin in impurity bound excitons.

**D. Excitation-dependent PL**

Luminescence excitation measurements probe higher excited states of the optical centers and are often used to reveal the recombination process that is giving rise to a particular peak. Excitation-dependent PL was performed for  ${}^a\text{Hf}^0$ ,  ${}^d\text{Hf}^0$ , and  ${}^e\text{Hf}^0$ . Figure 5 shows three possible types of radiative recombination processes. Transition "a" is conduction band-to-acceptor and "c" is donor-to-valence band. Transition "b" is a recombinative process between a donor level and an acceptor level, which results in donor-acceptor pair (DAP) emission. Donor-acceptor pair recombination has been well studied by Hopfield *et al.*,<sup>20</sup> Dean *et al.*,<sup>21</sup> and Lucovsky *et al.*<sup>22</sup> Through extensive review of experimental work,<sup>21</sup> the following five criteria<sup>22</sup> have become known to unambiguously identify lines of DAP origin.

- (1) The PL peak shifts to higher energies with increasing excitation intensity.
- (2) The PL peak narrows significantly with increasing excitation intensity.
- (3) The PL peak shifts towards higher energies with increasing donor concentration.
- (4) The PL peak intensity decreases rapidly above 35 K.
- (5) As the temperature increases, the PL peak shifts to higher energies.

We were able to investigate four (1, 2, 4, and 5) of these five conditions. Figure 6 shows the intensity of the 943.8 meV line ( ${}^a\text{Hf}^0$ ) with its two phonon replicas for various excitation intensities. As the excitation intensity is increased (see Fig. 6), the line does not shift to higher energies (criterion 1 fails) and the peak does not appear to narrow significantly (criterion 2 fails). In addition, it is evident from Fig. 7 that the intensity of the peak decreases gradually as the temperature reaches 35 K (criterion 4 fails) and the peak shifts to lower energy as the temperature is increased (criterion 5 fails). Testing conditions 1, 2, 4, and 5 indicates that the  ${}^a\text{Hf}^0$  peak does not appear to be a DAP transition.<sup>23</sup> In addition, excitation-dependent PL was measured on peaks labeled as  ${}^d\text{Hf}^0$  and  ${}^e\text{Hf}^0$  and are shown in Figs. 8 and 9, respectively.

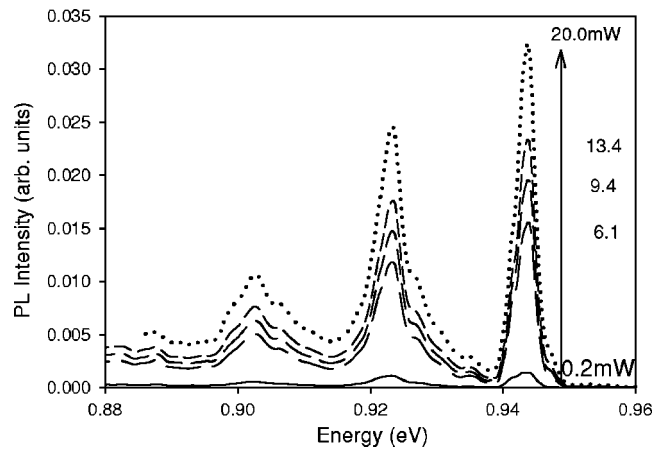


FIG. 6. PL spectrum of the  ${}^a\text{Hf}^0$  line (along with phonon replicas) under various excitation intensity from 0.2 to 20 mW measured at 12 K. The sample was annealed at 650 °C for 30 min, 1000 °C for 3 h, and rapidly quenched.

The laser power incident on the sample was varied from 0.45 to 20.9 mW. The peak labeled  ${}^d\text{Hf}^0$  in Fig. 8 neither appears to shift to higher energies nor shows band narrowing as the excitation power is increased. The same is true for the  ${}^e\text{Hf}^0$  peak in Fig. 9. This strongly suggests that none of the three emission lines studied in detail,  ${}^a\text{Hf}^0$ ,  ${}^d\text{Hf}^0$ ,  ${}^e\text{Hf}^0$ , is due to DAP transition.

The pressure dependence of the 845 meV PL line ( ${}^e\text{Hf}^0$ ) measured in the range up to 84 kbar (due to the background infrared luminescence of the diamond anvils available to us, only the shift of the strongest PL line in the slow cool sample could be measured) revealed that the peak shifts to lower energy with the pressure coefficient of approximately  $-0.045$  meV/kbar, which is much less than the pressure coefficients of the conduction band ( $-3.9$  meV/kbar) and the valence band ( $-2$  meV/kbar).<sup>24</sup> These data point towards the possibility that  ${}^e\text{Hf}^0$  could be an internal transition rather than a donor-to-band transition. Erbium in silicon is another well-known example of metal impurity with internal transition in a similar energy range. Although Er internal transition

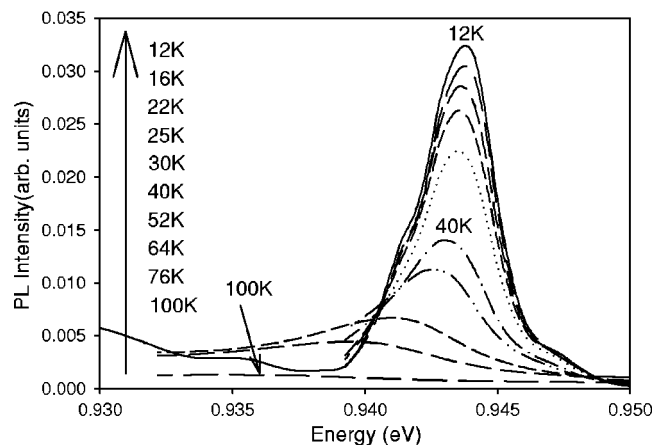


FIG. 7. PL spectrum of the  ${}^a\text{Hf}^0$  line measured under varying temperature from 12 to 100 K. The sample was annealed at 650 °C for 30 min, 1000 °C for 3 h, and rapidly quenched.

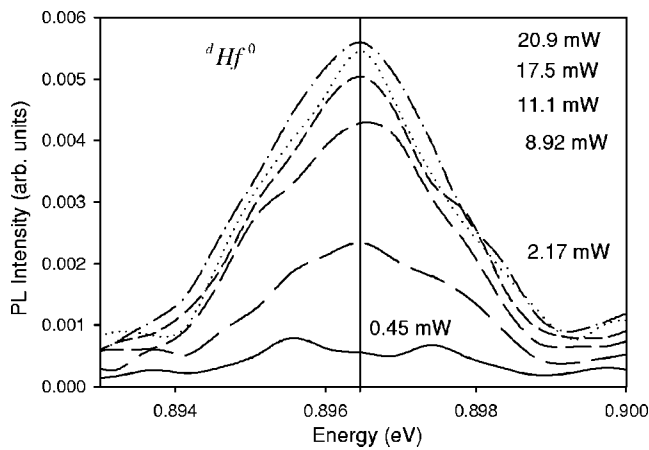


FIG. 8. PL spectrum of the  ${}^4d\text{Hf}^0$  line under various excitation intensity from 0.45 to 20.9 mW. The sample was annealed at 650 °C for 30 min, 1000 °C for 3 h, and slowly cooled.

of  $4f \rightarrow 4f$  ( $4I_{13/2} \rightarrow 4I_{15/2}$ , see Refs. 14, 15, and 25–28 for details) is not accompanied by phonon replicas,<sup>27</sup>  ${}^e\text{Hf}^0$  zero phonon line appears to have three of them. The observation of phonon replicas does not necessarily contradict the intrinsic nature of the transition, for example, Cr in GaAs has an internal transition ( ${}^3E \rightarrow {}^5T_2$ ) with phonon replicas.<sup>29–31</sup> The internal transition of Cr involves  $3d$  orbitals and  ${}^e\text{Hf}^0$  transition most likely involves its  $5d$  orbitals since the electronic configuration of Hf is  $4f^{14}5d^26s^2$ . Since the  $d$  orbitals are much less localized than the  $f$  orbitals, they interact with the host lattice stronger than the  $f$  orbitals, so coupling is possible, which in its turn leads to appearance of phonon replicas.

The energy level diagram<sup>32</sup> of the atomic transitions of Hf are shown in Fig. 10. We could not match the energy of the 845 meV transition (or any other transition listed in Table I) with the known optical transitions of Hf in vacuum, as it was done in the case of Er, unless we assumed that the energies of the  $d$  orbitals of Hf shift due to the presence of the crystal field of silicon. For example, in view of Fig. 10, the 814 meV ( $a^3P_1 \rightarrow a^3F_2$ ) transition would become 845 meV if  $a^3P_1$  shifts to higher energy by 31 meV.

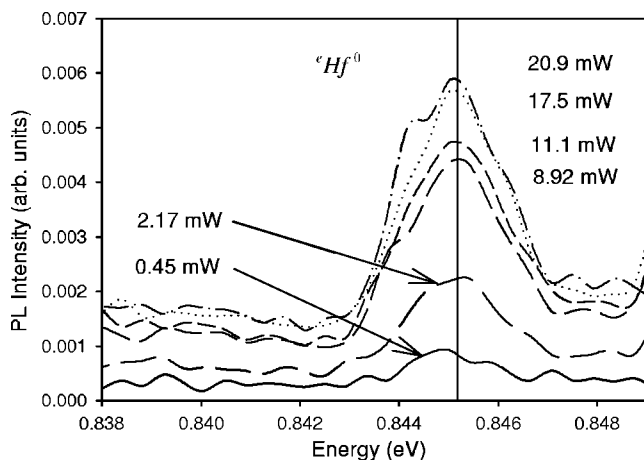


FIG. 9. PL spectrum of the  ${}^e\text{Hf}^0$  line under various excitation intensity from 0.45 to 20.9 mW. The sample was annealed at 650 °C for 30 min, 1000 °C for 3 h, and slowly cooled.

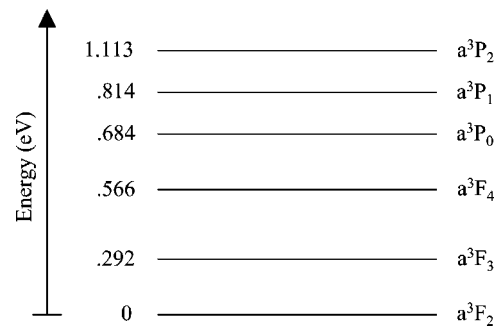


FIG. 10. Energy level diagram for the atomic transitions of Hf (from Ref. 32).

In the case of Er, which has a  $4f$  internal transition at the wavelength of 1.54  $\mu\text{m}$ , it was found that the luminescence peak appears at the same wavelength whether it is implanted in GaAs, GaP, or InP. We implanted Hf in GaAs at dose of  $10^{13} \text{ cm}^{-2}$  and energy of 87 keV, and annealed two samples following the procedure optimized by Gernot *et al.*<sup>33</sup> for luminescence of Er in GaAs [rapid thermal annealed in flowing forming gas (90%  $\text{N}_2$  and 10%  $\text{H}_2$ ) at 700 °C for 30 s]. However, no Hf-related PL signal was observed. This might indicate that either the temperature which worked well for Er in GaAs is insufficient for Hf in GaAs, or that a certain local environment is required to activate photoluminescence in the case of a less localized  $5d$  transition.

First, we will discuss the possibility that this PL signal is due to hafnium silicide. Hafnium easily forms bonds to silicon with the formation of hafnium silicide observed at temperatures as low as 450 °C.<sup>34–36</sup> However, the features of Hf-related photoluminescence are not characteristic for silicides. It is instructive to compare Hf-related PL at about 1.3  $\mu\text{m}$  with the 1.54  $\mu\text{m}$  luminescence that results from  $\beta\text{-FeSi}_2$  precipitates in Si.<sup>37,38</sup> Several important differences are evident. One is that the iron-silicide peak has a full width at half maximum (FWHM) of 52.6 meV for the iron implanted at an energy of 100 keV, whereas the  ${}^a\text{Hf}^0$  peak is much narrower and has a FWHM of only 3 meV or less. Second is that the iron implanted samples show one peak with no phonon replicas, whereas our Hf-implanted samples do show phonon replicas.<sup>38</sup> The excitation-dependent PL for the 100 keV Fe implant shows a shift in peak energy as a function of excitation power as opposed to our samples which show no shift in peak energy (see Figs. 6, 8, and 9). Finally, the temperature-dependent PL of  $\beta\text{-FeSi}_2$  shows hardly any drop in PL signal from 16–100 K,<sup>37</sup> but displays a three orders of magnitude drop between 100–200 K from which well-defined activation energy of 0.26 eV can be determined. From Fig. 4, it is clear that for Hf-PL, the signal shows a relatively insignificant drop from 12–20 K but shows a one order of magnitude drop from 20–100 K from which two activation energies, 8.95 and 85.4 meV, can be obtained. At 100 K the Hf-related PL signal disappears completely. Therefore, it is clearly evident from the differences presented above between the  $\beta\text{-FeSi}_2$  and the  ${}^a\text{Hf}^0$  that it is very unlikely that the Hf-related photoluminescence observed in our study originates from hafnium silicide precipitates in silicon.

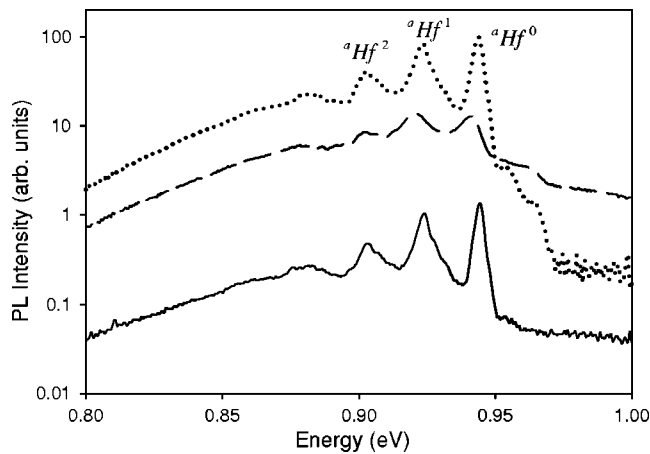


FIG. 11. PL spectra taken of Hf implanted in *n*-CZ silicon with coimplantation of oxygen at a dose of  $10^{13}$   $\text{cm}^{-2}$  (solid line),  $10^{14}$   $\text{cm}^{-2}$  (dashed curve), and  $10^{15}$   $\text{cm}^{-2}$  (dotted line). All samples were annealed at 650 °C for 30 min, 1000 °C for 3 h, and rapidly quenched.

#### E. Effect of oxygen on optical centers

It is well known that oxygen (O) enhances the luminescence of optical centers such as zinc<sup>17</sup> and erbium<sup>39,40</sup> in silicon. To check if oxygen would have a similar effect on the formation of Hf-related optical centers, Hf-implanted samples were coimplanted with oxygen. Three types of samples were used. Oxygen was coimplanted at an energy of 50 keV, 80° tilt, and dose of  $10^{13}$ ,  $10^{14}$ , and  $10^{15}$   $\text{cm}^{-2}$ . According to the SRIM (Ref. 41) simulation results, these implantation parameters ensured flat distribution of oxygen over the Hf-implanted area. The local implanted oxygen concentration at the peak of the implantation profile was calculated to be  $10^{18}$ ,  $10^{19}$ , and  $10^{20}$   $\text{cm}^{-3}$ . Since we used CZ silicon with background oxygen content around  $10^{18}$   $\text{cm}^{-3}$ , and Hf was implanted with  $\text{HfO}^-$  species, the local oxygen concentration at the Hf projected range depth could reach  $10^{18}$   $\text{cm}^{-3}$  even in the samples which were not coimplanted with oxygen. Additional oxygen implantation at dose of  $10^{13}$   $\text{cm}^{-2}$  did not change this concentration substantially; implantation at doses of  $10^{14}$  and  $10^{15}$   $\text{cm}^{-2}$  increased it by one and two orders of magnitude, respectively.

The oxygen-coimplanted samples were annealed in a horizontal furnace at 650 °C for 30 min, 1000 °C for 3 h, and then rapidly quenched. Figure 11 displays PL spectra measured for these samples. The solid, dashed, and dotted lines represent Hf samples coimplanted with oxygen at dose of  $10^{13}$ ,  $10^{14}$ , and  $10^{15}$   $\text{cm}^{-2}$ , respectively. Each of the curves in Fig. 11 was normalized relatively to the phosphorus bound exciton peak at 1091.8 meV.

Evidently, the intensity of the  $^a\text{Hf}^0$  line and its phonon replicas increases with the oxygen concentration (note that

the vertical scale in Fig. 11 is logarithmic). In fact, in the samples in which oxygen coimplantation increased the local oxygen concentration by two orders of magnitude, the PL intensity is also enhanced two orders of magnitude. Hence, it is clear that oxygen is involved, either directly or indirectly, in the formation of the observed Hf-related PL signal. A similar experiment was performed with slowly cooled sample; however, no strong impact of oxygen concentration on the PL intensity was observed in this case.

#### IV. CONCLUSIONS

A new Hf-related PL signature is reported. More than 25 lines and five sequences have been tabulated. The observation of these lines and their phonon replicas is dependent on the cooling conditions: most of the series appear after slow cooling from 1000 °C, whereas only five lines are observed after rapid quench. It was found that the “slow cool” PL spectrum can be converted into a “rapid quench” PL spectrum by reannealing the sample. Shift in the peak positions observed in samples implanted with two different isotopes of Hf provides evidence that the observed signal is Hf related. Temperature- and excitation-dependent PL of zero phonon lines  $^a\text{Hf}^0$ ,  $^d\text{Hf}^0$ , and  $^e\text{Hf}^0$  was performed. None of the three emission lines appears to be donor-acceptor pair transitions. It was concluded that the 943.8 meV ( $^d\text{Hf}^0$ ) line is most likely due to impurity exciton complex, whereas the 896.6 meV ( $^d\text{Hf}^0$ ) line seems to originate from impurity bound excitons. The calculated residual one-particle binding energy of 845 meV ( $^e\text{Hf}^0$ ) line seems to correlate with the energy level at  $E_C-0.27$  eV. The 896.6 meV ( $^d\text{Hf}^0$ ) emission line correlates with the energy position of the Hf-related deep level defect at  $E_C-0.22$  eV. The calculated residual one-particle binding energy of 943.8 meV ( $^a\text{Hf}^0$ ) line falls in the middle between the  $E_C-0.10$  eV and  $E_C-0.17$  eV deep levels, and therefore could not be matched exactly to either of these levels. The pressure measurements on  $^e\text{Hf}^0$  line suggest that it could be an internal transition within its *d* shell; however, neither the peak energy could be correlated with the known Hf optical transition in vacuum, nor could we observe the same transition in Hf-implanted GaAs. The PL intensity of Hf in rapidly quenched sample is enhanced in the presence of high oxygen concentration.

#### ACKNOWLEDGMENTS

We would like to thank J.Beeman for oxygen coimplantation, W.Shan for help with pressure measurements, H.Huff and P.Y.Yu for stimulating discussions, and H.Lemke for discussions and providing samples doped with Hf during growth. Helpful discussions and collaboration with O.F.Vyvenko is gratefully appreciated. The initial stages of this project were supported by Sematech.

\*Electronic mail: ravinder@berkeley.edu

- <sup>1</sup>S. J. Lee, H. F. Luan, C. H. Lee, T. S. Jeon, W. P. Bai, Y. Senzaki, D. Roberts, and D. L. Kwong, in *Symposium on VLSI Technology* (Japan Soc. Appl. Phys., 2001), p. 133.
- <sup>2</sup>G. D. Wilk and R. M. Wallace, *Appl. Phys. Lett.* **74**, 2854 (1999).
- <sup>3</sup>H. Lemke, *Phys. Status Solidi A* **122**, 617 (1990).
- <sup>4</sup>A. Claverie, B. Colombeau, G. B. Assayag, C. Bonafos, F. Cristiano, M. Omri, and B. de Mauduit, *Mater. Sci. Semicond. Process.* **3**, 269 (2000).
- <sup>5</sup>P. N. K. Deenapanray and M. Petracic, *J. Appl. Phys.* **85**, 3993 (1999).
- <sup>6</sup>P. N. K. Deenapanray and M. Petracic, *Surf. Interface Anal.* **29**, 160 (2000).
- <sup>7</sup>P. N. K. Deenapanray and M. Petracic, *J. Appl. Phys.* **87**, 2178 (2000).
- <sup>8</sup>P. N. K. Deenapanray and M. Petracic, *J. Vac. Sci. Technol. A* **19**, 893 (2001).
- <sup>9</sup>P. A. Stolk, H. J. Gossmann, D. J. Eaglesham, D. C. Jacobson, C. S. Rafferty, G. H. Gilmer, M. Jaraiz, J. M. Poate, H. S. Luftman, and T. E. Haynes, *J. Appl. Phys.* **81**, 6031 (1997).
- <sup>10</sup>K. G. McGuigan, M. O. Henry, E. C. Lightowers, A. G. Steele, and M. L. W. Thewalt, *Solid State Commun.* **68**, 7 (1988).
- <sup>11</sup>W. Weber, *Phys. Rev. B* **15**, 4789 (1977).
- <sup>12</sup>G. Nilsson and G. Nelin, *Phys. Rev. B* **6**, 3777 (1972).
- <sup>13</sup>F. Priolo, G. Franzo, S. Coffa, A. Polman, V. Bellani, A. Carnera, and C. Spinella, in *Materials Synthesis and Processing Using Ion Beams Symposium. Mater. Res. Soc. 1994*, edited by R. J. Culbertson, O. W. Holland, K. S. Jones, and K. Maex (Mater. Res. Soc., Pittsburgh, PA, 1994), pp. 397–408.
- <sup>14</sup>F. Priolo, G. Franzo, S. Coffa, A. Polman, S. Libertino, R. Barklie, and D. Carey, *J. Appl. Phys.* **78**, 3874 (1995).
- <sup>15</sup>S. Coffa, S. Lombardo, F. Priolo, G. Franzo, S. U. Campisano, A. Polman, and G. N. van den Hoven, *Nuovo Cimento Soc. Ital. Fis., D* **18D**, 1131 (1996).
- <sup>16</sup>J. Weber, H. Bauch, and R. Sauer, *Phys. Rev. B* **25**, 7688 (1982).
- <sup>17</sup>M. O. Henry, J. D. Campion, K. G. McGuigan, E. C. Lightowers, M. C. do Carmo, and M. H. Nazare, *Semicond. Sci. Technol.* **9**, 1375 (1994).
- <sup>18</sup>D. Bimberg, M. Sondergeld, and E. Grobe, *Phys. Rev. B* **4**, 3451 (1971).
- <sup>19</sup>F. E. Williams and H. J. Eyring, *J. Chem. Phys.* **15**, 289 (1947).
- <sup>20</sup>J. J. Hopfield, D. G. Thomas, and M. Gershenson, *Phys. Rev. Lett.* **10**, 162 (1963).
- <sup>21</sup>P. J. Dean, *Progress in Solid State Chemistry* (Pergamon, New York, 1973), Vol. 8, p. 1.
- <sup>22</sup>G. Lucovsky, A. J. Varga, and R. F. Schwartz, *Solid State Commun.* **3**, 9 (1965).
- <sup>23</sup>G. D. Gilliland, *Mater. Sci. Eng., R.* **18**, 99 (1997).
- <sup>24</sup>W. Su-Huai and A. Zunger, *Phys. Rev. B* **60**, 5404 (1999).
- <sup>25</sup>S. Coffa, G. Franzo, F. Priolo, A. Polman, and R. Serna, *Phys. Rev. B* **49**, 16 313 (1994).
- <sup>26</sup>P. G. Kik, A. Polman, S. Libertino, and S. Coffa, *J. Lightwave Technol.* **20**, 834 (2002).
- <sup>27</sup>H. Ennen, G. Pomrenke, A. Axmann, K. Eisele, W. Haydl, and J. Schneider, *Appl. Phys. Lett.* **46**, 381 (1985).
- <sup>28</sup>H. Ennen, J. Schneider, G. Pomrenke, and A. Axmann, *Appl. Phys. Lett.* **43**, 943 (1983).
- <sup>29</sup>B. Deveaud, G. Picoli, Y. Zhou, and G. Martinez, *Solid State Commun.* **46**, 359 (1983).
- <sup>30</sup>B. Deveaud, G. Picoli, B. Lambert, and G. Martinez, *Phys. Rev. B* **29**, 5749 (1984).
- <sup>31</sup>T. Nishino, in *Defect and Impurity Engineered Semiconductors and Devices. Symposium. Mater. Res. Soc. 1995*, edited by S. Ashok, J. Chevallier, I. Akasaki, N. M. Johnson, and B. L. Sopori (Mater. Res. Soc., Pittsburgh, PA, 1995), pp. 263–272.
- <sup>32</sup>C. E. Moore, *Atomic Energy Levels as Derived from the Analyses of Optical Spectra*, Natl. Bur. Stand. (U.S.) Circ. No. 32 (U.S. GPO, Washington, D.C., 1971).
- <sup>33</sup>G. S. Pomrenke, H. Ennen, and W. Haydl, *J. Appl. Phys.* **59**, 601 (1986).
- <sup>34</sup>J. Y. Cheng and L. J. Chen, *J. Appl. Phys.* **68**, 4002 (1990).
- <sup>35</sup>J. Y. Cheng and L. J. Chen, *Appl. Phys. Lett.* **56**, 457 (1990).
- <sup>36</sup>S. Zaima, N. Wakai, T. Yamauchi, and Y. Yasuda, *J. Appl. Phys.* **74**, 6703 (1993).
- <sup>37</sup>C. Spinella, S. Coffa, C. Bongiorno, S. Pannitteri, and M. G. Grimaldi, *Appl. Phys. Lett.* **76**, 173 (2000).
- <sup>38</sup>Y. Maeda, Y. Terai, M. Itakura, and N. Kuwano, *Thin Solid Films* **461**, 160 (2004).
- <sup>39</sup>K. Nakashima, O. Eryu, O. Iioka, H. Minami, and M. Watanabe, in *Rare Earth Doped Semiconductors II*, edited by S. Coffa, A. Polman, and R. N. Schwartz (Mater. Res. Soc., Pittsburgh, PA, 1996), p. 75.
- <sup>40</sup>D. L. Adler, D. C. Jacobson, D. J. Eaglesham, M. A. Marcus, J. L. Benton, J. M. Poate, and P. H. Citrin, *Appl. Phys. Lett.* **61**, 2181 (1992).
- <sup>41</sup>J. F. Ziegler, J. P. Biersack, and U. Littmark, (Pergamon Press, New York, 1985), p. 321.